# Microstructural properties of over-doped GaN-based diluted magnetic semiconductors grown by MOCVD*

Tao Zhikuo(陶志阔)[1,2], Zhang Rong(张荣)[1,†], Xiu Xiangqian(修向前)[1,†], Cui Xugao(崔旭高)[1], Li Li(李丽)[3], Li Xin(李鑫)[1], Xie ZiLi(谢自力)[1], Zheng Youdou(郑有炓)[1], Zheng Rongkun(郑荣坤)[3], and Simon P Ringer[3]

[1]Key Laboratory of Advanced Photonic and Electronic Materials, School of Electronic Science and Engineering, Nanjing University, Nanjing 210093, China
[2]College of Electronic Science and Engineering, Nanjing University of Posts and Telecommunications, Nanjing 210003, China
[3]Australia Key Center for Microscopy and Microanalysis, University of Sydney, Sydney, NSW 2006, Australia

**Abstract:** We have grown transition metal (Fe, Mn) doped GaN thin films on *c*-oriented sapphire by metal-organic chemical vapor deposition. By varying the flow of the metal precursor, a series of samples with different ion concentrations are synthesized. Microstructural properties are characterized by using a high-resolution transmission electron microscope. For Fe over-doped GaN samples, hexagonal $Fe_3N$ clusters are observed with $Fe_3N$ (0002) parallel to GaN (0002) while for Mn over-doped GaN, hexagonal $Mn_6N_{2.58}$ phases are observed with $Mn_6N_{2.58}$(0002) parallel to GaN (0002). In addition, with higher concentration ions doping into the lattice matrix, the partial lattice orientation is distorted, leading to the tilt of GaN (0002) planes. The magnetization of the Fe over-doped GaN sample is increased, which is ascribed to the participation of ferromagnetic iron and $Fe_3N$. The Mn over-doped sample displays very weak ferromagnetic behavior, which probably originates from the $Mn_6N_{2.58}$.

**Key words:** MOCVD; DMS; high-resolution TEM
**DOI:** 10.1088/1674-4926/33/7/073002 **EEACC:** 2520

## 1. Introduction

The combination of ferromagnetism with semiconducting properties in a III–V semiconductor makes it a promising material for future applications of spintronics. Some successes in preparing materials have been achieved. For instance, ferromagnetic Mn-doped InAs and Mn-doped GaAs with $T_C$ above 110 K have been obtained[1]. However, from the viewpoint of applications, the $T_C$ of Mn-doped III-As materials falls short of the expected values. Compared to these Mn-doped III-As materials, ferromagnetic DMS materials with $T_C$ above room temperature are desirable for practical applications. According to mean-field theory based on Zener's model of ferromagnetism, the Curie temperature of p-type Mn-doped GaN could exceed room temperature, under the condition that the material has a Mn concentration of 5% and $3.5 \times 10^{20}$ holes/cm$^3$ which is necessary for carrier-mediated exchange[2]. This prediction inspired great interest in the research into GaN-based DMSs. A variety of techniques were employed to prepare Mn-doped GaN, including solid-state diffusion[3], MBE[4,5], ion implantation[6] and MOCVD[7−13]. However, the experimental results of magnetism in Mn-doped GaN are highly controversial. Both ferromagnetism and paramagnetism in Mn-doped GaN were reported. In addition, Fe-doped GaN has also been explored and the exhibited magnetic behaviors are not yet understood. Using the ion-implantation method, Fe-doped GaN showed ferromagnetic behavior with bcc-Fe nanoclusters[14] or without observation of secondary phases[15,16]. Also, Fe ions were introduced into GaN by the MOCVD method during film growth, and ferromagnetic behaviors were observed[17−20]. It has also been presented by Ref. [18] that two kinds of Fe-rich regions exist in (Ga, Fe)N: spinodal decomposition, which does not involve the participation of another crystallographic phase, $\varepsilon$-$Fe_3N$ nanoclusters or Fe nanoclusters. These two components all contribute to the exhibited magnetic properties. However, no convincing proof has ever been presented by anyone to prove that homogenous Mn or Fe-doped GaN is ferromagnetic up to now. The origin of the exhibited ferromagnetic characteristics is still under investigation. It is probably due to the homogeneous behavior of the alloy, or rather originates from ferromagnetic clusters imbedded in the host GaN.

In this paper, we focus on the microstructural properties of over-doped GaN based DMSs with Fe or Mn doping grown by the MOCVD technique. The correlation between the structure and the exhibited magnetic behaviors has been discussed. The microstructure and crystalline quality of films were analyzed by HRTEM. Both the plane and the cross-sectional views were investigated. Cross-sectional samples were prepared using a conventional sandwich technique. The specimens were

* Project supported by the Special Funds for Major State Basic Research Project, China (No. 2011CB301900), the Hi-Tech Research Project, China (No. 2009AA03A198), the National Natural Science Foundation of China (Nos. 60990311, 60820106003, 608201060, 60906025, 60936004, 61106009), the Natural Science Foundation of Jiangsu Province, China (Nos. BK2008019, K2009255, BK2010178, BK2010385), and the Research Funds from NJU-Yangzhou Institute of Opto-Electronics.
† Corresponding author. Email: rzhang@nju.edu.cn; xqxiu@nju.edu.cn
Received 30 January 2012, revised manuscript received 27 February 2012

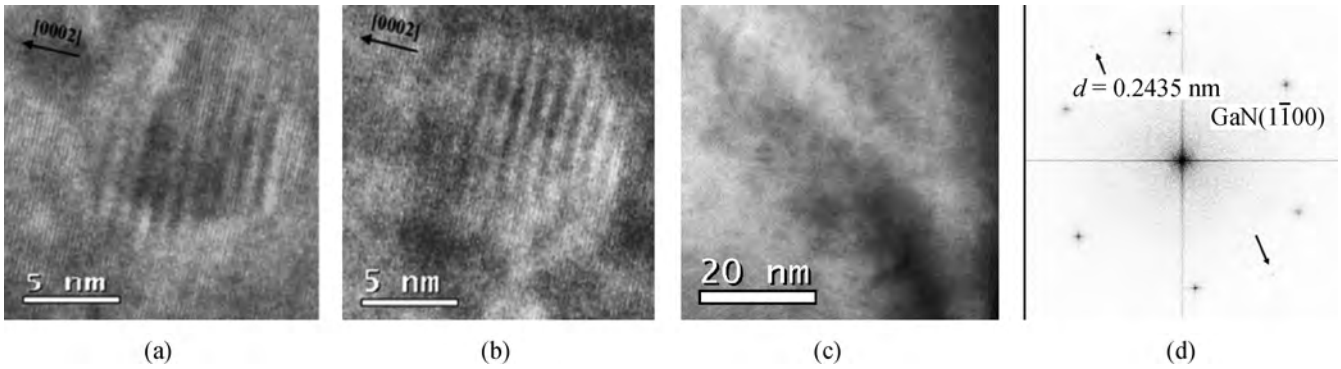


Fig. 1. (a), (b) Cross-sectional TEM images of $Ga_{0.99}Fe_{0.01}N$. (c) Plane-view TEM image of $Ga_{0.96}Mn_{0.04}N$ and (d) the corresponding FFT image.

first thinned mechanically and then $Ar^+$ ion milling was applied as the final stage of thinning. All TEM observations were carried out with a JEOL JEM-3000F system operated at an accelerating voltage of 300 kV.

## 2. Experimental procedures

The epilayers in this work were grown by conventional MOCVD with a horizontal reaction chamber. The $c$-sapphire substrates put on graphites were heated by radio frequency (RF). The undoped GaN layers used as the templates were grown at 1050 ℃ followed by the growth of doped GaN epilayers at 1050 ℃ (for Fe-doped samples) or 900 ℃ (for Mn-doped samples). Trimethylgallium (TMGa), bis(cyclopentadienyl)iron ($Cp_2Fe$), bis(methylcyclopentadienyl)manganese ($MCp_2Mn$) and ammonia ($NH_3$) were used as the gallium, iron, manganese, and nitrogen precursors, respectively. The other growth conditions were as follows: a reactor pressure of 76 Torr, $H_2$ carrier gas, the bubbler temperature of +40 ℃ for both $Cp_2Fe$ and $MCp_2Mn$. The concentration of Fe in the films was varied up to 1% (the mole fraction was estimated by using energy dispersive spectrometry) by controlling the molar flow ratios of the precursors while the Mn concentration increased up to 4%. The doped GaN layer is about 1 $\mu$m thick and all of the films had a semi-insulating property.

## 3. Results and discussion

By using the X-ray diffraction (XRD) technique, our previous work on $Ga_{1-x}Fe_xN$ ($x$ denoted mole fraction of cations) has shown that no second phase is detected for all samples with $x < 1\%$, while precipitations are detected for sample $Ga_{0.99}Fe_{0.01}N$[21]. The peaks ascribed to the (0002) reflection of $\varepsilon$-$Fe_3N$, the (10$\bar{1}$0) reflection of $\varepsilon$-Fe and the (110) reflection of $\alpha$-Fe, respectively, were observed. Although the peak corresponding to $\varepsilon$-$Fe_3N$ (0002) is very weak, the precipitation of $Fe_3N$ has been detected definitely through TEM measurement and this will be discussed with the TEM results.

For cross-sectional images of $Ga_{0.99}Fe_{0.01}N$, the enclosure nano precipitations are observed directly. Figures 1(a) and 1(b) are cross-sectional images of the $Ga_{0.99}Fe_{0.01}N$ sample. As shown in the images, the enclosure precipitations of Figs. 1(a) and 1(b) are identified as $\varepsilon$-$Fe_3N$ and the observed Moiré fringes are interpreted by the overlapping of GaN (0002) planes and $Fe_3N$ (0002) planes. It can be calculated that the $d$-spacing related to planes of nano precipitations along the growth orientation are 0.226 nm and 0.222 nm, which are ascribed to the (0002) planes of $\varepsilon$-$Fe_3N$[19]. Many other $\varepsilon$-$Fe_3N$ precipitations of similar size have been observed in images from different locations of the sample, and we can evaluate the average value for the diameter to be about 15 nm. It was also suggested by Ref. [18] that the precipitation occurs by a nucleation mechanism in which only nanocrystals with a critical size can form.

Based on the previous XRD and demonstrated TEM results, it is suggested that hexagonal $Fe_3N$ could be formed in our Fe over-doped GaN sample during growth. Significantly, $Fe_3N$ precipitations are also $c$-oriented in the $c$-oriented GaN matrix. However, $Fe_3N$ has not been observed for $Ga_{0.99}Fe_{0.01}N$ in the plane-view images and this may be due to the fact that the precipitations exist with $Fe_3N$ (0002) parallel to GaN (0002) planes. Both $Fe_3N$ and GaN belong to the h.c.p. crystal group, and, more importantly, the lattice mismatch between the $Fe_3N$ (0002) and GaN (0002) planes is about –1.8%, which makes the precipitations difficult to observe from the plane-view image[22]. Although $\varepsilon$-Fe and $\alpha$-Fe phases are detected in the XRD spectra, we have not found them in TEM images. According to another report, the detectible Fe phase by XRD may exist close to the surface due to nitrogen evaporation at the growing surface[19] or exist in the surface due to the Fe segregation[23]. Even though we have achieved several HRTEM images over large areas, no other structure of second-phase or metal-cluster segregation was observed directly. However, the HRTEM can only detect an extremely tiny area at a time and so the possibility of the existence of other phases still cannot be excluded.

For our $Ga_{1-x}Mn_xN$ samples, previous work has shown that no other participate has been detected by XRD with $x \leqslant 2.7\%$ while an unconfirmed $Mn_xN_y$ phase has been observed in $Ga_{0.96}Mn_{0.04}N$ with a wide and weak peak at a $2\theta$ value of around 36.5°[12, 13]. Combined with the following TEM results, it is suggested that this peak is ascribed to the (0002) reflection of hexagonal $Mn_6N_{2.58}$. Figure 1(c) is the lower magnification TEM plane-view image of $Ga_{0.96}Mn_{0.04}N$ and Figure 1(d) is the corresponding fast Fourier transformation (FFT) image. Besides the spots relating to the $c$-oriented hexagonal GaN lattice, another really weak spot is observed, as indicated

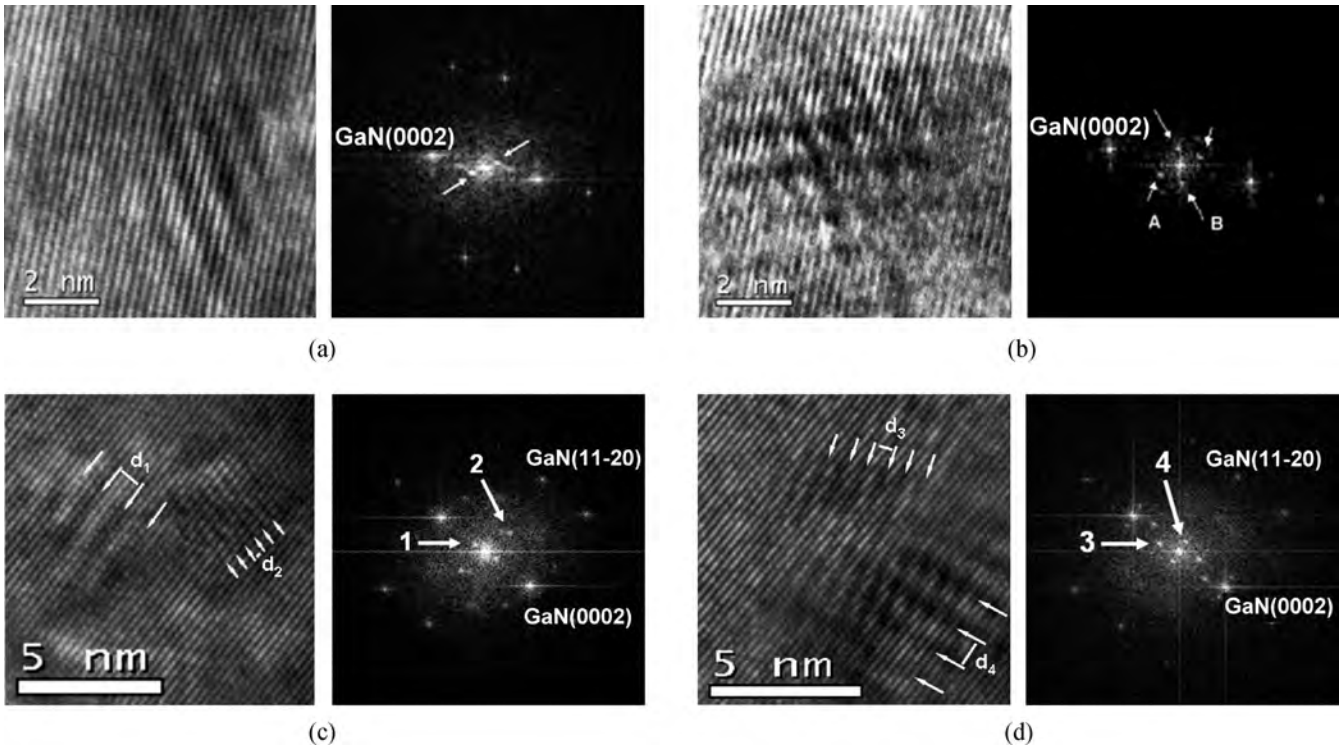


Fig. 2. Cross-sectional HRTEM images and corresponding FFT images of (a, b) $Ga_{0.99}Fe_{0.01}N$ and (c, d) $Ga_{0.96}Mn_{0.04}N$.

by the arrows. Using $a_{GaN} = 0.3189$ nm, the calculated distance of lattice planes related to this spot is 0.2435 nm, and this group of planes is considered to be the $(11\bar{2}0)$ planes of $Mn_6N_{2.58}$, the lattice of which is hexagonal with $a = 0.4891$ nm and $c = 0.4554$ nm. Although $Mn_6N_{2.58}$ precipitations have not been observed directly from the HRTEM images, it is suggested that $Mn_6N_{2.58}$ could be formed in our Mn over-doped GaN samples. Significantly, the embedded hexagonal $Mn_6N_{2.58}$ would be also $c$-oriented in the $c$-oriented GaN matrix. In this view, it is suggested that by using the MOCVD method, the doping level of Fe in homogenous $Ga_{1-x}Fe_xN$ is less than 1% and that of Mn in $Ga_{1-x}Mn_xN$ is less than 4%.

Meanwhile, clear zipper-like features are observed in both of the over-doped GaN samples ($Ga_{0.99}Fe_{0.01}N$ and $Ga_{0.96}Mn_{0.04}N$) by HRTEM. Figures 2(a) and 2(b) are cross-sectional images of $Ga_{0.99}Fe_{0.01}N$ while Figures 2(c) and 2(d) are cross-sectional images of $Ga_{0.96}Mn_{0.04}N$. In Fig. 2, clear zipper-like features related to the Moiré fringes caused by two sets of GaN (0002) planes with a small angle $\theta$ between them can be seen. The $\theta$ can be determined by the following equation:

$$\theta = \frac{1}{2}\arcsin\frac{d_{(0002)}}{2d_{\text{moire}}}, \tag{1}$$

where $d_{(0002)}$ is the lattice distance of the GaN (0002) plane, while $d_{\text{moire}}$ is the period distance of the Moiré fringe which can be determined by the TEM image or by FFT spots. Using Eq. (1), we can determine $\theta = 4.0°$ in Fig. 2(a). In Fig. 2(b), two sets of Moiré fringes are observed, which are marked A and B as the arrows point in the corresponding FFT image, and we can also determine the $\theta$ value of 4.8° and 3.9°, respectively. As shown in Figs. 2(c) and 2(d), many more Moiré fringes are observed for sample $Ga_{0.96}Mn_{0.04}N$. Following the same procedure, we can get $\theta_1 = 4.09°$, $\theta_2 = 8.68°$, $\theta_3 = 6.38°$, $\theta_4 = 3.20°$, and it is also noticeable that $\theta_2 \approx 2\theta_1$, $\theta_3 \approx 2\theta_4$. By using the scheme shown in Fig. 3, it is clear that Moiré fringes $d_1$ and $d_4$ are formed by the tilting of the GaN (0002) plane to the mother lattice with the angle $\theta$, while fringes $d_2$ and $d_3$ are formed by two tilted GaN (0002) planes with the angle $2\theta$ between them.

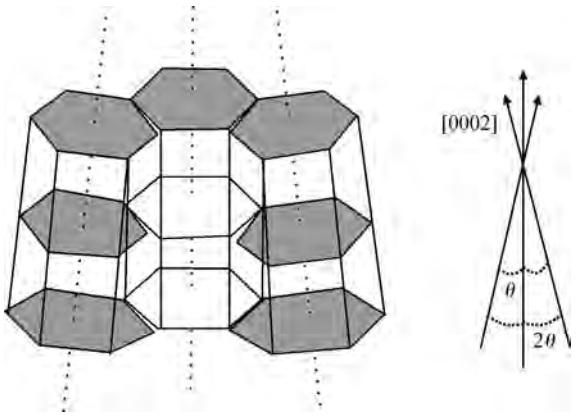


Fig. 3. Scheme of the tilted GaN planes.

Based on the above discussion, it is suggested that precipitations are formed in over-doped GaN based DMSs. Meanwhile, an over amount of ion doping decreases the crystal quality of the sample and makes partial areas of the GaN lattice distorted, which leads to the tilting of GaN (0002) planes. It is also the reason why other XRD diffraction peaks not corresponding to $c$-oriented GaN (such as GaN $(1\bar{1}00)$) have usually been observed in over-doped GaN based DMSs films grown on $c$-sapphire[21].

In view of the above results, the correlation between the structure and magnetic behaviors has also been discussed. For different $Ga_{1-x}Fe_xN$ samples, clear hysteresis is visible in every magnetization versus the field curve, which means all of the samples show room temperature ferromagnetic behaviors[21]. Through increasing the Fe doping concentration, the magnetization changes from 0.50, 0.74 to 1.40 emu/cm$^3$ for $Ga_{0.9908}Fe_{0.002}N$, $Ga_{0.9905}Fe_{0.005}N$ and $Ga_{0.99}Fe_{0.01}N$, respectively. The magnetization of the over-doped $Ga_{0.99}Fe_{0.01}N$ sample increases a lot, which is ascribed to the participation of ferromagnetic iron and $Fe_3N$ as previous XRD and the presented TEM results indicate. Meantime, we can see that (Ga,Fe)N materials exhibit ferromagnetic behaviors even without other crystallographic phases detected. Moreover, the average concentration of iron ions is far below the percolation limit of the nearest neighbor coupling, and at the same time the free carrier density is too low to mediate an efficient long-range exchange interaction. So, the origin of the ferromagnetic behaviors could not be ascribed to the double-exchange interactions or carrier-mediated exchange interactions, and this still needs more indisputable results. For our $Ga_{1-x}Mn_xN$ samples, paramagnetic behaviors have been observed for $x \leqslant 2.7\%$ while very weak ferromagnetic behavior can be observed for over-doped $Ga_{0.96}Mn_{0.04}N$[12]. As the above results indicate, $Mn_6N_{2.58}$ has been observed in $Ga_{0.96}Mn_{0.04}N$. So it is suggested that the observed weak ferromagnetism may probably originate from $Mn_6N_{2.58}$.

## 4. Conclusion

We have grown Fe-doped GaN and Mn-doped GaN film by using the MOCVD method with different concentrations of Fe and Mn ions. The results show that our grown homogeneous $Ga_{1-x}Mn_xN$ films are not ferromagnetic, while the $Ga_{1-x}Fe_xN$ films are ferromagnetic, and, most importantly, hexagonal Fe or a Mn nitride phase are easily formed during the film growth with the $c$-axis parallel to the $c$-axis of hexagonal GaN. However, the origin of the exhibited magnetism still can not been determined definitely and more convincing experimental results are required in order to confirm our results.

## References


[1] Matsukura F, Ohno H, Shen A, et al. Transport properties and origin of ferromagnetism in (Ga,Mn)As. Phys Rev B, 1998, 57: R2037

[2] Dietl T, Ohno H, Matsukura F, et al. Zener model description of ferromagnetism in zinc-blende magnetic semiconductors. Science, 2000, 287: 1019

[3] Reed M L, El-Masry N A, Stadelmaier H H, et al. Room temperature ferromagnetic properties of (Ga, Mn)N. Appl Phys Lett, 2001, 79: 3473

[4] Thaler G T, Overberg M E, Gila B, et al. Magnetic properties of n-GaMnN thin films. Appl Phys Lett, 2002, 80: 3964

[5] Sonoda S, Shimizu S, Sasaki T, et al. Molecular beam epitaxy of wurtzite (Ga,Mn)N films on sapphire (0001) showing the ferromagnetic behaviour at room temperature. J Cryst Growth, 2002, 237–239: 1358

[6] Theodoropoulou N, Hebard A F, Overberg M E, et al. Magnetic and structural properties of Mn-implanted GaN. Appl Phys Lett, 2001, 78: 3475

[7] Reed M J, Arkun F E, Berkman E A, et al. Effect of doping on the magnetic properties of GaMnN: Fermi level engineering. Appl Phys Lett, 2005, 86: 102504

[8] Arkun F E, Reed M J, Berkman E A, et al. Dependence of ferromagnetic properties on carrier transfer at GaMnN/GaN:Mg interface. Appl Phys Lett, 2004, 85: 3809

[9] Kane M H, Strassburg M, Fenwick W E, et al. Correlation of the structural and ferromagnetic properties of $Ga_{1-x}Mn_xN$ grown by metalorganic chemical vapor deposition. J Cryst Growth, 2006, 287: 591

[10] Kane M H, Asghar A, Vestal C R, et al. Magnetic and optical properties of $Ga_{1-x}Mn_xN$ grown by MOCVD. Semicond Sci Technol, 2005, 20: L5

[11] Strassberg J, Kane M H, Asghar A, et al. The Fermi level dependence of the optical and magnetic properties of $Ga_{1-x}Mn_xN$ grown by MOCVD. J Phys: Condens Matter, 2006, 18: 2615

[12] Cui X G, Tao Z K, Zhang R, et al. Structural and magnetic properties in Mn-doped GaN grown by MOCVD. Appl Phys Lett, 2008, 92: 152116

[13] Cui X G, Zhang R, Tao Z K, et al. Optical and structural properties of Mn-doped GaN grown by MOCVD. Chin Phys Lett, 2009, 26: 038103

[14] Talut G, Reuther H, Grenzer J, et al. Spinodal decomposition and secondary phase formation in Fe-oversaturated GaN. Phys Rev B, 2010, 81: 155212

[15] Theodoropoulou N, Hebard A F, Chu S N G, et al. Characterization of high dose Fe implantation into p-GaN. Appl Phys Lett, 2001, 79: 3452

[16] Shon Y, Lee S, Jeon H C, et al. Origin of clear ferromagnetism for p-type GaN implanted with $Fe^+$. Appl Phys Lett, 2006, 89: 082505

[17] Kane M H, Gupta S, Fenwick W E, et al. Comparative study of Mn and Fe incorporation into GaN by metalorganic chemical vapor deposition. Phys Status Solidi A, 2007, 204: 61

[18] Bonanni A, Kiecana M, Simbrunner C, et al. Paramagnetic GaN:Fe and ferromagnetic (Ga,Fe)N: the relationship between structural, electronic, and magnetic properties. Phys Rev B, 2007, 75: 125210

[19] Li T, Simbrunner C, Navarro-Quezada A, et al. Phase-dependent distribution of Fe-rich nanocrystals in MOVPE-grown (Ga,Fe)N. J Cryst Growth, 2008, 310: 3294

[20] Bonanni A, Navarro-Quezada A, Li T, et al. Controlled aggregation of magnetic ions in a semiconductor: an experimental demonstration. Phys Rev Lett, 2008, 101: 135502

[21] Tao Z K, Zhang R, Cui X G, et al. Optical and magnetic properties of Fe-doped GaN DMSs prepared by MOCVD method. Chin Phys Lett, 2008, 25: 1476

[22] Tao Z K, Cui X G, Zhang R, et al. Epitaxial growth of ferromagnetic $Fe_3N$ films on GaN(0002) substrates by MOCVD method. J Cryst Growth, 2010, 312: 1525

[23] Balmer R S, Soley D E J, Simons A J, et al. On the incorporation mechanism of Fe in GaN grown by metal-organic vapour phase epitaxy. Phys Status Solidi C, 2006, 3: 1429